Visible photoluminescence from nanostructured Si-based layers produced by air optical breakdown on silicon

A. V. Kabashin[a] and M. Meunier
Laser Processing Laboratory, Department of Engineering Physics, Ecole Polytechnique de Montréal, Case Postale 6079, succ. Centre-ville, Montréal (Québec) H3C 3A7, Canada

(Received 19 February 2002; accepted 6 January 2003)

Pulsed radiation of CO_2 laser has been used to produce an optical breakdown on a silicon target in atmospheric air. After several breakdown initiations near the threshold of plasma production, a highly porous layer was formed under the radiation spot on the silicon surface. The fabricated layers presented the porosity of 75%–80% and were formed of silicon nanocrystals imbedded in SiO_2 matrix. They exhibited strong photoluminescence (PL) around 2.0 eV, which was stable to a prolonged continuous illumination of samples. Possible mechanisms of nanostructure formation and PL origin are discussed. © *2003 American Institute of Physics.* [DOI: 10.1063/1.1557752]

Nanostructured Si-based materials are in the focus of numerous studies for the last decade (see, e.g., Refs. 1–13). They are known to exhibit visible photoluminescence (PL) with quantum efficiency of up to a few percent, although crystalline silicon has a small (1.11 eV at room temperature) and indirect band gap. The luminescent property opens up possibilities for creating Si-based photonics devices and their integration in standard silicon microelectronics technology.

Due to good compatibility with silicon processing technology, ''dry'' fabrication techniques are considered as the most adequate and promising for optoelectronics applications. These techniques generally imply a deposition of a thin nanostructured film on a substrate, as, for example, in experiments with magnetron sputtering,[2] plasma deposition,[3] laser breakdown of silane,[4] pulsed laser ablation.[5–7] However, in some cases it is important to produce local nanostructured area directly on a silicon-based device or an assembled integrated chip. One of the possibilities is a local annealing by pulsed radiation from an excimer laser of an amorphous Si-based film below the plasma initiation threshold.[8,9] Another possibility is the electric spark processing of a silicon wafer.[10–13] In particular, the spark-processed material was found to exhibit strong PL in UV/blue (3.22 eV) and green (2.36 eV) spectral ranges and relatively weak and unstable PL in the red (1.9 eV) range.[13]

In this letter, we demonstrate another dry and vacuum-free method for the local patterning of photoluminescent nanostructured Si-based materials on a silicon wafer. A phenomenon of air optical breakdown[14] produced by focusing IR radiation on silicon is used to modify the silicon surface transforming it to a nanostructured layer.

The optical breakdown was produced on a silicon target by the radiation of a pulsed TEA CO_2 laser (wavelength 10.6 μm, pulse energy 1 J, pulse length 1 μs FWHM, repetition rate 3 Hz). The radiation was focused by a Fresnel's lens with the focal length of 5 cm, giving the radiation intensity of about 10^8 W/cm^2 at the focal plane. Standard silicon wafers (*n*- and *p*-type, resistance 0.01–10 Ω cm) with dimensions about 1×1 cm^2 were used as targets. Experiments were carried out in atmospheric air (1 atm, 20 °C, 40% humidity). The PL spectra were recorded on a double spectrometer (U100, Instruments SA) using 488 nm radiation of an Ar^+ laser with power density of 30 W/cm^2 as a source and a GaAs photomultiplier as the detector. Scanning electron microscopy (SEM), x-ray diffraction (XRD), and specular x-ray reflectivity[15] (SXRR) spectroscopies were used to examine structural properties of the films. In addition, x-ray photoemission spectroscopy (XPS) was used to determine the surface layer composition. After the breakdown ignition, the plasma intensity raised progressively with the number of laser shots and stabilized only after 10–20 shots. The intensity gain was apparently connected to the appearance of mechanical defects on the target surface, which improved the radiation absorption. Our experiments were carried out near the threshold of plasma production to minimize the size of treated area.

After the breakdown initiations by several laser pulses, a gray-tint area was formed under the focal spot on the silicon surface. The processed area exhibited strong PL signals, which could be easily seen by naked eyes. Figure 1 shows that a typical PL spectrum had the emission band in red range around 2.0 eV. The peak position was independent of a number of breakdown initiations, silicon wafer type (*n*- or *p*-) and its doping level. The PL signals were relatively stable to a prolonged illumination of the layers by the Ar^+ laser radiation. In particular, the decrease of their integral intensity did not exceed 40% even after 6 h of the continuous illumination. Surface examination by SEM did not reveal the presence of microscale spikes on the treated surface, as in experiments with silicon processing by 800-nm fs (Ref. 16) or UV ns (Ref. 17) radiation. In contrast, the treated area represented a highly porous material containing holes and cracks, as one can see in Fig. 2(a). The size of holes was between 30 and 150 nm [Fig. 2(b)], but smaller holes, not resolved by SEM, may still be additionally present. A prolonged treatment of the silicon surface by 100–200 pulses could lead to the additional formation of channels with similar dimensions. Nevertheless, the mean size of holes and channels did not change with the number of laser shots. Our study showed that redeposition of material outside the irradiation spot was

[a]Electronic mail: akabach@email.phys.polymtl.ca

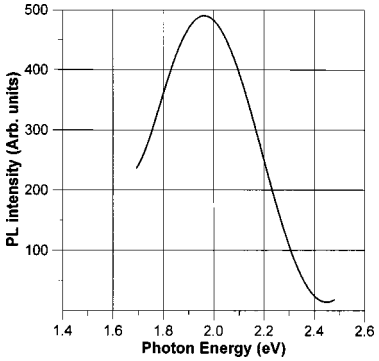

FIG. 1. Typical photoluminescence spectrum from the central part of Si-based layer fabricated by the breakdown processing of a silicon wafer [*p*-type, (1,0,0), 0.01 Ω cm] by 100 laser shots at the same focal spot.

very weak. Even after 200–400 laser pulses, we did not detect the formation of a film of the redeposited material just around the spot, as one usually observes with conventional laser ablation.[5,7] However, isolated microscale particles could be present after a large number of breakdown initiations (100–150 laser pulses). These particles probably originated from large-scale material fragments, which cracked from the target after its prolonged breakdown treatment.

The layer porosity was estimated from SXRR[15] spectra. They were obtained with the use of an x-ray diffractometer, which made possible a monitoring of the intensity of x-ray beam ($\lambda = 0.154$ nm) reflected from a sample under a simultaneous θ–2θ scanning of a source and a detector ($0° < \theta < 1°$, θ was measured towards the surface). Since for x rays the refractive index of most materials is less than 1, a total external reflection occurs for $\theta < \theta_c$, while for $\theta > \theta_c$ the reflected intensity suffers a rapid attenuation. Taking into account that θ_c is proportional to the square root of the material density,[15] the porosity can be determined from the critical angle measurements by the following formula:

$$\text{porosity}(\%) = 100\left(1 - \frac{\theta_c^2}{\theta_{c\ \text{bulk Si}}^2}\right), \tag{1}$$

where θ_c and $\theta_{c\ \text{bulk Si}}$ are the critical angles for a thin film and bulk silicon, respectively.

Experimental reflectivity curves for a silicon target before and after the treatment are presented in Fig. 3. One can see that the critical angle $\theta_{c\ \text{bulk Si}}$ for the substrate before the treatment (curve 1) was about 0.22°, which is in agreement with previous studies.[18] However, the treatment led to the appearance of an additional angle θ_c at about 0.1°–0.11° (curve 2) associated with the air/layer interface. Substituting the values of $\theta_{c\ \text{bulk Si}}$ and θ_c into Eq. (1), we obtain the layer porosity of 75%–80%. The precision of SXRR measurements was about 10%.

As shown in Fig. 4, the XPS spectrum of the target before the treatment was characterized by a strong peak at −99.8 eV and a relatively weak one at −103.5 eV, which are assigned to the Si $2p$ photoelectrons of the unoxidized Si core and the natural SiO_x oxide layer, respectively. The treatment led to a disappearance of Si-related peak, while the oxide-related peak became stronger and shifted to higher energies up to 104 eV. The latter peak is always assigned to pure SiO_2, suggesting that the processed layer mainly consisted of SiO_2. Nevertheless, XRD studies showed that Si crystals were also present in the layer. Figure 5(a) shows typical spectra for the silicon target before and after the optical breakdown processing. One can see that the treatment led to the appearance of additional XRD peaks around 28.45° and 47.3°, which are associated with crystalline silicon planes (1,1,1) and (2,2,0), respectively. This gives the evidence that the resulting layers consisted of silicon crystals embedded in SiO_2 matrix. It is known[19] that the broadness of XRD peaks is mainly determined by the smallest clusters in a deposit. As the instrumental noises are relatively low, this property could be used to estimate the minimal size of crystals in the deposit by the Debye–Scherrer formula.[19] Taking the broadness of a typical silicon peak [$\Delta(2\theta)/2 = 0.6°$] from a highly resolved XRD spectrum [Fig. 5(b)], the estimation gives the crystal size of the order of 10 nm.

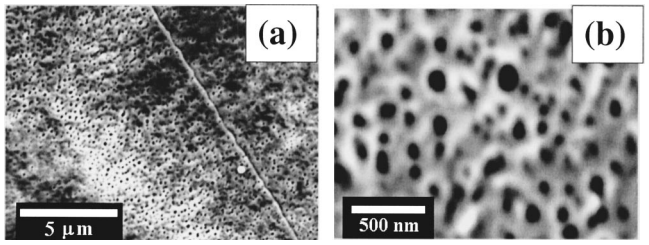

FIG. 2. Typical SEM images of a silicon target surface under the radiation spot after ten breakdown initiations.

It is well known that the interaction of the CO_2 laser radiation with matter is characterized by a strong photon absorption by the plasma itself.[14] The target serves to generate initial electrons then, the formed plasma develops in the cold gas toward the focusing lens and absorbs main IR radiation power at its shock wave forefront through the inverse Bremsstrahlung mechanism. As a result, the plasma gets heated up to temperatures of about 10^4 K, while the radiation power on the target surface decreases dramatically and the radiation-related ablation of material drops.[14] After the laser pulse, the plasma decays gradually during milliseconds and is characterized by the presence of intense currents (with magnitudes up to 10^6 A)[20] and various electromagnetic effects.[21–23] In our opinion, the action of radiation leads to a localized melting and even flash evaporation of the target material. This process probably takes place only in some casual points, which causes the appearance of pores on the target surface. The laser-ablated material and the upper target layer are then heated by the hot CO_2 laser-induced breakdown plasma or its currents during milliseconds, leading to additional phase transformations and the initiation of chemical reactions in the plasma. Since the radiation is pulsed, one can assume recrystallization or local vapor redeposition of the material during the off times. The combined action of laser- and plasma-related processes gives rise to a modification of properties of Si-based compounds formed on the surface and their nanostructuring. The mechanism of surface treatment in our experiments seems to be similar in many respects to that of the electric spark processing.[10–13] The spark-processed silicon also contained 10–500 nm holes and consisted of silicon nanocrystals embedded in SiO_2 matrix. The surface modifications were attributed to pulsed ion bombardment of silicon, which led to a flash evaporation of the material and its re-

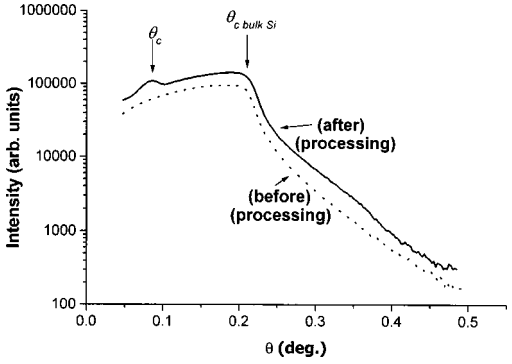

FIG. 3. Typical SXRR spectra before (spectrum 1) and after (2) the breakdown processing. To enhance SXRR signal, a rectangular area with dimensions of 5×5 mm^2 was treated on a silicon wafer by shifting the laser beam over the target. Each point of the area was treated by at least 100 laser pulses.

crystallization during the off times. The layers fabricated by the electric spark processing in pure oxygen exhibited similar 1.9 eV signals,[10,11,13] though they were relatively weak and fast degrading.[13] However, there is no consensus on the origin of these signals. The generation of 1.9 eV PL band is frequently ascribed to defects in SiO_2 structure.[24,25] However, detailed analysis of similar 1.9 eV signals and their properties in the case of spark-processed silicon does not confirm this assumption.[12,13] Some properties of 1.9 eV signals such as the degradation behavior were attributed to a radiative relaxation of excited oxygen atoms originating from the dissociation of ozone molecules,[13] whereas other properties give evidence for the mechanism of a radiative recombination between quantum confined states in the nanoscale particles.[11] In any case, a clear identification of the PL mechanism requires further detailed study of mechanical, structural, and PL properties of the deposited and annealed films. These investigations are in progress.

In summary, air optical breakdown has been produced on a silicon target for local nanostructuring of its material. We showed that the breakdown production led to the formation of porous layer under the radiation spot, which consisted of silicon nanocrystals imbedded in a SiO_2 matrix and exhibited strong red PL. This method can be used for a controlled local patterning of photoluminescent nanostructured materials.

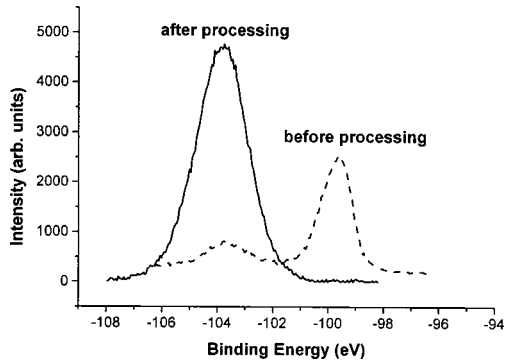

FIG. 4. Typical XPS spectra before (spectrum 1) and after (2) the breakdown processing.

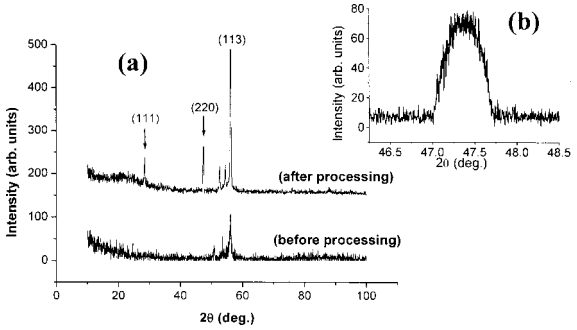

FIG. 5. (a) Typical XRD spectra before (spectrum 1) and after (1) the breakdown processing of a silicon wafer [*n*-type, (1,0,0), 10 Ω cm]. The later spectrum was collected from the treated area with the dimensions 5×5 mm^2; (b) highly resolved XRD spectrum near a crystalline silicon line.

The authors are grateful to R. Leonelli for assistance during PL studies, and to S. Poulin for the XPS measurements. We also acknowledge the financial contribution from the Natural Science and Engineering Research Council of Canada.

[1] L. T. Canham, Appl. Phys. Lett. **57**, 1046 (1990).
[2] H. Takagi, H. Ogawa, Y. Yamazaki, A. Ishizaki, and T. Nakagiri, Appl. Phys. Lett. **56**, 2379 (1990).
[3] Y. Kanemitsu, T. Ogawa, K. Shiraishi, and K. Takeda, Phys. Rev. B **48**, 4883 (1993).
[4] E. Edelberg, S. Bergh, R. Naone, M. Hall, and B. S. Aydil, Appl. Phys. Lett. **68**, 1415 (1996).
[5] I. A. Movtchan, R. W. Dreyfus, W. Marine, M. Sentis, M. Autric, G. Le Lay, and N. Merk, Thin Solid Films **255**, 286 (1995).
[6] Y. Yamada, T. Orii, I. Umezu, Sh. Takeyama, and T. Yoshida, Jpn. J. Appl. Phys., Part 1 **35**, 1361 (1996).
[7] A. V. Kabashin, J.-P. Sylvestre, S. Patskovsky, and M. Meunier, J. Appl. Phys. **91**, 3248 (2002).
[8] K. M. A. El-Kader, J. Oswald, J. Koka, and V. Chab, Appl. Phys. Lett. **64**, 2555 (1994).
[9] Z. Wang, J. Li, X. Huang, L. Wang, J. Xu, and K. Chen, Solid State Commun. **117**, 383 (2001).
[10] R. E. Hummel and S.-S. Chang, Appl. Phys. Lett. **61**, 1965 (1992).
[11] E. F. Steigmeier, H. Auderset, B. Delley, and R. Morf, J. Lumin. **57**, 9 (1993).
[12] R. E. Hummel, A. Morrone, M. Ludwig, and S.-S. Chang, Appl. Phys. Lett. **63**, 2771 (1993).
[13] M. H. Ludwig, A. Augustin, and R. E. Hummel, Semicond. Sci. Technol. **12**, 981 (1997).
[14] Yu. P. Raizer, *Laser-Induced Discharge Phenomena* (Consultants Bureau, New York, 1977).
[15] L. T. Parratt, Phys. Rev. **95**, 359 (1954).
[16] T.-H. Her, R. J. Finlay, C. Wu, S. Deliwala, and E. Mazur, Appl. Phys. Lett. **73**, 1673 (1998).
[17] A. J. Pedraza, J. D. Fowlkes, and D. H. Lowndes, Appl. Phys. Lett. **74**, 2322 (1999).
[18] M. Tolan, Springer Tracts Mod. Phys. **148**, 7 (1999).
[19] B. D. Cullity, *Elements of X-ray Diffraction* (Addison-Wesley, Reading, MA, 1978).
[20] M. G. Drouet and H. Pepin, Appl. Phys. Lett. **28**, 426 (1976).
[21] V. V. Korobkin and R. V. Serov, Pis'ma Zh. Eksp. Teor. Fiz. **4**, 103 (1966) [JETP Lett. **4**, 70 (1966)].
[22] A. V. Kabashin and P. I. Nikitin, Quantum Electron. **27**, 536 (1997).
[23] A. V. Kabashin, P. I. Nikitin, W. Marine, and M. Sentis, Appl. Phys. Lett. **73**, 25 (1998).
[24] S. Munekuni, T. Yamanaka, Y. Shimogaichi, K. Nagasawa, and Y. Hama, J. Appl. Phys. **68**, 1212 (1990).
[25] D. L. Griscom, J. Ceram. Soc. Jpn. **99**, 923 (1991).